Renal Energy Metabolism Following Acute Dichloroacetate and 2,4-Dinitrophenol Administration: Assessing the Cumulative Action with Hyperpolarized [1-^{13}C]Pyruvate MRI

Lotte Bonde Bertelsen, Per Mose Nielsen, Haiyun Qi, Christian Østergaard Mariager, Jakob Lindhardt, and Christoffer Laustsen

MR Research Centre, Department of Clinical Medicine, Aarhus University, Aarhus, Denmark

Corresponding Author:
Christoffer Laustsen, PhD
Palle Juul-Jensens Boulevard 99, 8200 Aarhus N, Denmark;
E-mail: cl@clin.au.dk

Key Words: MRI, hyperpolarization, DCA, 2,4-DNP, metabolism
Abbreviations: 2,4-Dinitrophenylhydrazine (2,4-DNP), pyruvate dehydrogenase kinase (PDK), dichloroacetate (DCA), pyruvate dehydrogenase (PDH), magnetic resonance imaging (MRI), magnetic resonance (MR), normal rat kidney (NRK)

ABSTRACT

Numerous patient groups receive >1 medication and as such represent a potential point of improvement in today's healthcare setup, as the combined or cumulative effects are difficult to monitor in an individual patient. Here we show the ability to monitor the pharmacological effect of 2 classes of medications sequentially, namely, 2,4-dinitrophenol, a mitochondrial uncoupler, and dichloroacetate, a pyruvate dehydrogenase kinase inhibitor, both targeting the oxygen-dependent energy metabolism. We show that although the 2 drugs target 2 different metabolic pathways connected ultimately to oxygen metabolism, we could distinguish the 2 in vivo by using hyperpolarized [1-^{13}C]pyruvate magnetic resonance imaging. A statistically significantly different pyruvate dehydrogenase flux was observed by reversing the treatment order of 2,4-dinitrophenol and dichloroacetate. The significance of this study is the demonstration of the ability to monitor the metabolic cumulative effects of 2 distinct therapeutics on an in vivo organ level using hyperpolarized magnetic resonance imaging.

INTRODUCTION

Renal hypoxia is associated with a high likelihood of developing renal disease; in fact, it is considered a unifying mechanism in the development of renal disease (1-4). Renal hypoxia has a plethora of origins, and one such origin is mitochondrial uncoupling, which has been shown to lead to end-stage renal disease, even in the absence of additional co-mediators of renal disease such as hyperglycemia (2, 5).

Although mitochondrial uncoupling is considered a protective mechanism, as an antioxidant system, and has been shown to improve diabetic symptoms in mice, its co-occurrence with increased oxygen consumption leads to renal hypoxia (6-8).

Renal hypoxia, originating from treatment with the weight loss/slimming aid 2,4-Dinitrophenylhydrazine (2,4-DNP), known for its adverse significant effects (9), has been shown to mimic many of the early signs of diabetic renal disease (5). To date, no current treatments exist that reverse the renal metabolic and functional deterioration seen in many patients with diabetes (10).

Thus, new therapeutics regimes targeting renal hypoxia or the associated metabolic maladaptations are of great interest. One such therapy/treatment is the pyruvate dehydrogenase kinase (PDK) inhibitor, dichloroacetate (DCA), an activator of pyruvate dehydrogenase (PDH) (11). PDH is a key enzyme that modulates glucose oxidation and mitochondrial NADH (nicotinamide adenine dinucleotide) production, which could alter the accelerated aerobic glycolytic phenotype during hypoxia by decreasing lactate accumulation. The stimulation of the mitochondrial function (increased oxidation of alanine and lactate) has been shown to improve tricarboxylic acid cycle flux as well as reduce the glucose levels in diabetes (12). Similar to DCA, activation of PKM2 (pyruvate kinase muscle isozyme M2), increases the pyruvate production and, in turn, increases the tricarboxylic acid cycle flux, and has shown similar protective mechanism during hyperglycemia (13).

Recently hyperpolarized [1-^{13}C]pyruvate magnetic resonance imaging (MRI) has been shown as a method for early identification of metabolic alterations following DCA treatment (11). Interestingly, DCA treatment supported the treatments mentioned in previous reports of diabetes, that is, the balance of myocardial substrate selection is restored, diastolic dysfunction is reversed, and even the blood glucose level in a type-2 rat model of diabetic cardiomyopathy is normalized (11).

In the liver and kidney, on the other hand, DCA has been reported to blunt gluconeogenesis, by reducing the lactate-to-pyruvate ratio with increasing DCA concentrations (14). This is

ISSN 2379-1381 http://dx.doi.org/10.18383/j.tom.2018.00022

opposite to the recent reports in which hyperpolarized MRI has been used, showing increased lactate production in the liver and kidney associated with the inhibition of gluconeogenesis by means of metformin (15-17). Interestingly, a similar increased lactate production has been associated with diabetes, originating from both a pseudohypoxic state (increased lactate production even under normoxic conditions) (18-21), largely determined by mitochondrial uncoupling (22), and increased gluconeogenesis (23). Thus we question if [1-^{13}C]pyruvate can differentiate a hyperglycemia-independent mitochondrial uncoupling phenotype (dinitrophenol-induced hypoxia) (5) from a gluconeogenesis inhibition phenotype (DCA treatment), and second, if a preconditioning effect of acute hypoxia is imposed by 2,4-DNP. This is particularly important, as many patients rely on several medications, and thus, the cumulative effects of these are a major concern when changing treatment regimens or designing clinical studies (24, 25). Increasingly, data suggest that combined effects of drugs can improve efficacy and simultaneously reduce the doses of individual compounds used and thus reduce the side effects (26-28). This originates from the fact that the individual effects of a single pharmacological drug and the cumulative effects of the combinations with other drugs or treatments might considerably alter the pharmacological response.

Central to tailored therapeutic treatment is the ability to monitor the effects of treatment, preferably with a noninvasive and sensitive method (29, 30). To date, no single method has ideally suited for the investigation of these combinations in vivo. This calls for new methods, allowing detailed metabolic examination of the various drug combinations on an organ level.

MATERIALS AND METHODS

In Vivo Examination

Ten 8-week-old female Wistar rats, weighing ~220 g, were included in this study. They were randomly divided into 2 treatment groups, with 5 rats in each. Two rats were excluded owing to technical difficulties during the examination. The rats were kept in standard cages under the following conditions: 12:12 h light:dark cycle, 21°C ± 2°C temperature; and 55% ± 5% humidity. All rats had free access to water and standard rat chow throughout the study. The rats were anesthetized with 2.5% sevoflurane in 2 L/min of air. A tail vein catheter (0.4 mm) was inserted to inject hyperpolarized [1-^{13}C] pyruvate, polarized in a 5 T SPINLab (GE Healthcare, Broendby, Denmark) as previously described (17).The magnetic resonance (MR) examinations were performed in a 3.0 T clinical MR system (GE Healthcare) equipped with a dual tuned ^{13}C/^{1}H volume rat coil (GE Healthcare) as described in the Nielsen et al. study (31). A section-selective ^{13}C IDEAL (iterative decomposition of water and fat with echo asymmetry and least-squares estimation) spiral sequence was used for the hyperpolarized [1-^{13}C]pyruvate imaging (21, 32). In short, a dynamic image series covering both kidneys in an 15-mm axial section every 5 seconds was acquired with the sequence parameters (flip angle = 10°, IDEAL echoes = 11, initial spectrum per IDEAL encoding = 1, repetition time = 100 milliseconds, echo time = 0.9 milliseconds, ΔTE = 0.9 milliseconds, field of view = 80 × 80 mm^2, and real resolution = 5 × 5 mm) (21). The body temperature was maintained around 37°C, and respiration and peripheral capillary oxygen saturation levels were monitored throughout the experiment. Acquired ^{1}H and ^{13}C images were converted to DICOM and analyzed in OsiriX (33). Following a baseline [1-^{13}C]pyruvate scan, either DCA (30 mg/mL, with 1 mL in 10 seconds and 0.5 mL over 15 minutes) or 2,4-DNP (15 mg/kg of 7.4 mg/mL solution) was administered intravenously and followed by the other compound in a crossover design (Figure 1). All procedures regarding this experiment were in compliance with the guidelines for use and care of laboratory animals. The study was approved by the Danish Inspectorate of Animal Experiments.

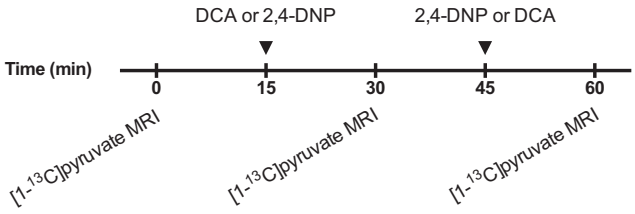

Figure 1. Time line. Experimental time line of the hyperpolarized examination. Three consecutive [1-^{13}C]pyruvate examinations were performed to estimate the changes associated with treatment with 2,4-Dinitrophenylhydrazine (2,4-DNP) and dichloroacetate (DCA) and their cumulative combination.

Rat Proximal Tubuli Cells

NRK52E (normal rat kidney: NRK) cells were grown in a humidified atmosphere of 5% CO_2–95% O_2 at 37°C in Dulbecco's Modified Eagle's Medium with low glucose (Sigma-Aldrich, Brondby, Denmark) supplemented with 10% fetal bovine serum, penicillin, and streptomycin. The growth medium was changed every second or third day. When cells reached 80% confluence, they were subcultured until further measurements.

Oxygen Consumption Rate

Oxygen consumption was measured at 37°C in a closed Micro-Respiration chamber with an O_2-electrode (Unisense A/S, Aarhus, Denmark). For each experiment, 10 million NRK cells were used. Peptides/Protein levels were measured using a Qubit 3.0 flourometer (Fisher Scientific, Slangerup, Denmark).

NRK cells were harvested by trypsination and resuspended in Dulbecco's Modified Eagle's Medium buffer before microrespiratory measurements. Cells were transferred to a closed chamber and allowed to stabilize for 5 minutes before the start of measurements. The treatment schedule shown in Table 1 was fulfilled, and each step had a duration of 5 minutes. DCA was used in a concentration of 10 mM and 2,4-DNP in a concentration of 0.1 mM. The adenosine triphosphate synthase was inhibited in the presence of 5 μM of oligomycin (34). Maximum respiratory capacity was measured in the presence of the uncoupler carbonyl cyanide m-chlorophenylhydrazone (CCCP) (2–3 titration steps of 0.05 μM) (34). Nonmitochondrial oxygen con-

Table 1. Oxygen Consumption Rate

	Basal Respiration	Treatment 1	Treatment 2	Oligomycin	CCCP	Antimycin-A	Rotenone
DCA–DNP treated	X	10 mM DCA	0.1 mM DNP	X	X	X	X
DNP–DCA treated	X	0.1 mM DNP	10 mM DCA	X	X	X	X

sumption processes was measured using rotenone (1 μM) and antimycin A (5 μM) to completely shut down the oxidative phosphorylation process (34).

Statistics

All data are presented as mean ± SEM. All statistical analyses were performed in GraphPad Prism 7 (GraphPad Software, Inc., La Jolla, CA). Data were analyzed by either an unpaired Student *t* test or with a 2-way or a 3-way repeated-measures ANOVA. A value of $P < .05$ (*) was considered statistically significant.

RESULTS

We examined the individual effects of the mitochondrial uncoupler 2,4-DNP and the PDK inhibitor DCA, as well as the combined effects in a crossover experiment (Figures 2 and 3). The cumulative effects of the 2 drugs were denoted as "DCA + 2,4-DNP" for the rats and cells receiving DCA before 2,4-DNP (Figure 3). Rats and cells receiving 2,4-DNP before DCA were denoted as "2,4-DNP + DCA". Both DCA and 2,4-DNP altered all metabolic pathways (pyruvate-to-lactate, pyruvate-to-alanine, and pyruvate-to-bicarbonate) investigated using hyperpolarized [1-^{13}C]pyruvate (blue bars in Figure 3A), with a statically significant difference between the overall treatment metabolic patterns ($P < .0001$). A general upregulation was seen with 2,4-DNP treatment, while DCA lowered the metabolic conversion compared with baseline measurements (Figure 3A). Furthermore, the cumulative treatment order (interaction term, time × treatment) was likewise found to be statistically significantly different between the 2 groups ($P = .0008$). The overall interaction term (metabolites × time × treatment), was not found to be significantly different between the 2 groups ($P = .6$). To determine if the observed changes with hyperpolarized [1-^{13}C]pyruvate reflect those in local oxygen availability, cell experiments we conducted to investigate the effects on oxygen consumption in proximal tubular cells. A similar overall treatment effect ($P = .01$) and cumulative interaction effects ($P = .01$) were observed, showing a significantly increased oxygen consumption of 90% following administration of 2,4-DNP (mitochondrial uncoupling), which was sustained following DCA treatment (increased PDH flux). DCA had little impact on the basal oxygen consumption; however, the addition of 2,4-DNP increased the oxygen consumption to 80%. No differences were seen in proton leakage or adenosine triphosphate production, while a numerical reduction of 50% was seen in the cumulative maximum respiration in the DCA + 2,4-DNP group, albeit a statistically different variation was seen in this group ($P = .01$) (Figure 4).

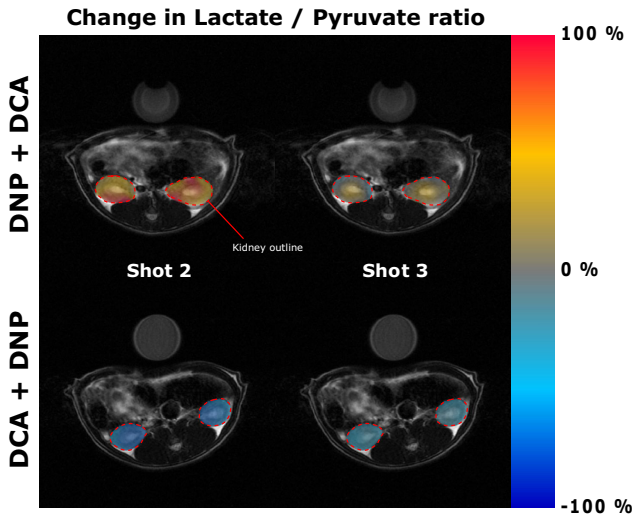

Figure 2. Representative images of the ^{13}C lactate-to-pyruvate signal changes. The lactate/pyruvate changes associated with the treatment with either 2,4-DNP and then afterwards DCA (top row) or DCA and then 2,4-DNP (bottom row). The color bar represents the change from baseline.

DISCUSSION

The main finding of this study is the radically different cumulative effect of combining a PDK inhibitor and a mitochondrial uncoupler, depending only on the timing of the 2 drugs and, second, the ability for hyperpolarized [1-^{13}C]pyruvate to monitor this acute cumulative effect in vivo.

The importance of this is derived from the fact that many patients benefit from >1 medication and/or treatments, and as a result, detailed knowledge of the immediate interplay between ≥2 medications or treatments, can help improve the treatment outcome. This can be achieved by reducing the needed medications or by improving the efficacy by selecting the optimum treatment pattern and timing. This study is, to best of the authors' knowledge, the first demonstration of the ability to monitor the cumulative effects of drugs in vivo using hyperpolarized MR.

The metabolic effects seen in vivo with hyperpolarized [1-^{13}C]pyruvate are corroborated by the striking similarities between the bicarbonate production (surrogate for oxidative phosphorylation) in rats and the oxygen consumption rate in proximal tubuli cells.

Although numerical difference was observed in the endpoint lactate and alanine production, it did not reach statistical significance. The importance of these potential metabolic differences is currently unknown, as we did not follow the long-term effects nor do we know if these patterns are essential for the

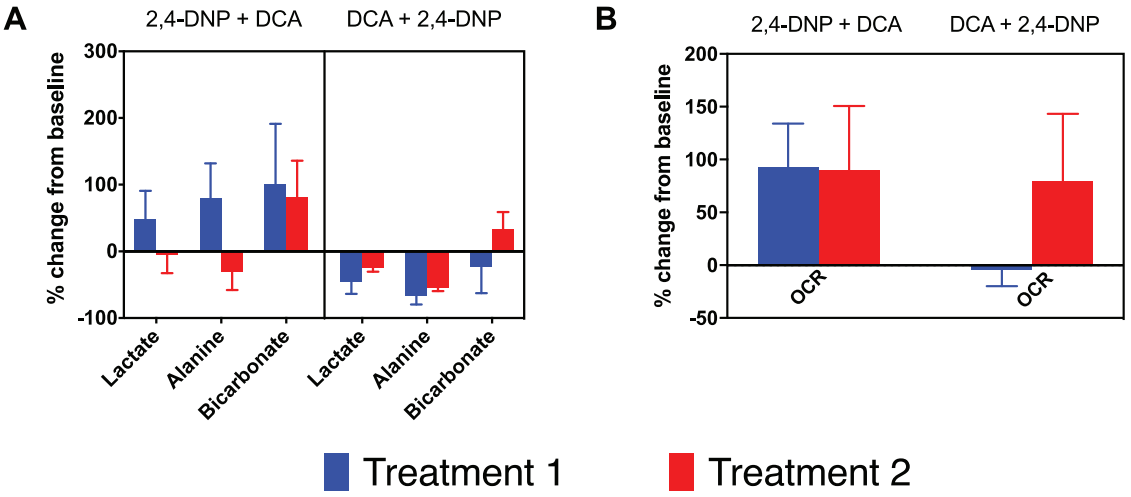

Figure 3. The comparison of metabolic pathways and oxygen consumption alterations associated with cumulative treatment with 2,4-DNP and DCA. The hyperpolarized metabolic profile and the treatment pattern of lactate, alanine, and bicarbonate normalized to pyruvate was both significantly different ($P < .0001$) (A). No difference was found with respect to time alone ($P = .13$), the interaction terms (metabolite × treatment) ($P = .56$), (metabolite × time) ($P = .9$), and (metabolite × treatment × time) ($P = .6$). However the effect of treatment with time (treatment × time) was found to be significantly different ($P = .0008$). A significant effect was observed in the basal respiration over time ($P = .01$), but not cumulative between the 2 treatment patterns ($P = .13$) (B). A significant interaction term (time x treatment) was seen ($P = .01$). The data are represented as mean ± SD.

renal outcome of the cumulative treatment of the 2 drugs. Furthermore, the dosing of both DCA and 2,4-DNP could potentially impose different effects depending of the doses used, and as such, the findings and interpretations in this study are limited to the specific dose regimes used here. However the ability to monitor these potential intermediary effects of additive treatment patterns directly in the organs in vivo hold great promise to improve the treatment efficacy in clinical settings. This is particularly true, as many patients are undergoing several treatments and thus potential improvement in efficacy, solely relying on the order and time window of the administration can be tested with hyperpolarized [1-^{13}C]pyruvate MRI. The individual effects of either DCA alone or 2,4-DNP alone were significantly different, showing a markedly increase in metabolic conversion following 2,4-DNP, while DCA decreased or maintained the lactate, alanine, and bicarbonate production. These findings supports earlier results showing that some doses of DCA may blunt gluconeogenesis, resulting in a reduction in the pyruvate-to-lactate ratio (14), while treatment with 2,4 DNP creates a hyperglycemia-independent mitochondrial uncoupling phenotype with increased lactate production and an increased mitochondrial oxygen consumption (5).

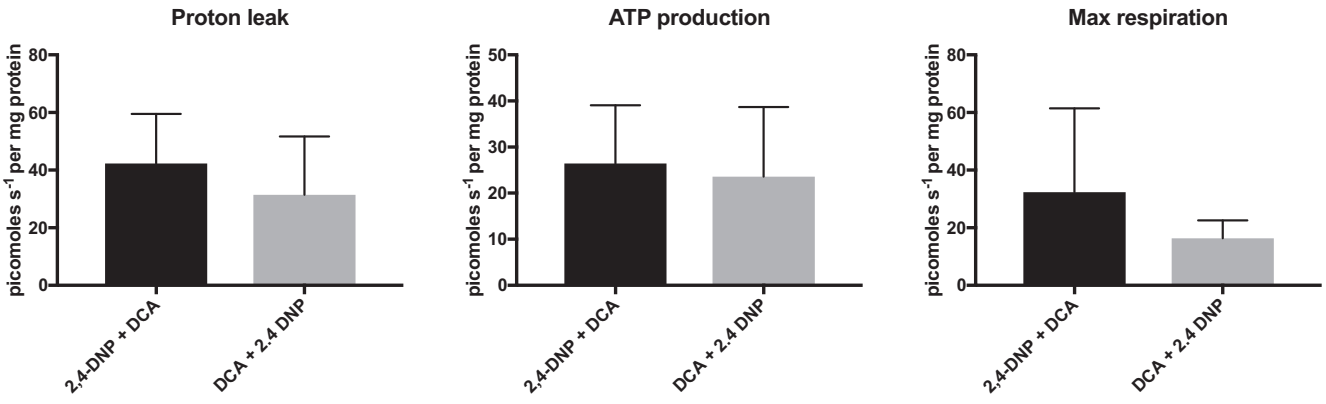

Figure 4. Individual parameters for proton leak, maximal respiration, and adenosine triphosphate (ATP) production. Proton leak is the difference in oxygen consumption rate (OCR) after oligomycin injection and antimycin A/rotenone. Maximal respiration is the OCR after carbonyl cyanide m-chlorophenylhydrazone (CCCP) injection and antimycin A/rotenone. ATP production is the difference in OCR before and after oligomycin. The data are represented as mean ± SEM.

This study highlights the power of hyperpolarized MR to investigate complex treatment regimes; however, the injection of supra-physiological concentrations of substrates should be considered a pharmacological challenge in this setting and caution of the translation of the results is necessary.

Recent reports have shown that liver-targeted mitochondrial uncoupling using a newly developed DNP derivative improves insulin sensitivity (8). This indicates a potentially better tolerated treatment using mitochondrial uncouplers in diabetes patients. Thus, future studies are needed to investigate the link between the improved metabolic flux seen in this study and the outcome on preventing, or even reversing, renal disease progression. This study supports the use of hyperpolarized MR to investigate the efficacy of these new drugs in both preclinical and clinical examinations. This is particularly true, as patients with diabetes today are typically already receiving multiple medications before the inclusion in drug trials.

ACKNOWLEDGMENTS

The study was supported by Aarhus University Research Foundation. Duy Anh Dang is acknowledged for his laboratory assistance.

Disclosure: No disclosures to report.

Conflict of Interest: The authors have no conflict of interest to declare.

REFERENCES

1. Aukland K, Krog J. Renal oxygen tension. Nature. 1960;188:671.
2. Brownlee M. Biochemistry and molecular cell biology of diabetic complications. Nature. 2001;414:813–820.
3. Fine LG, Orphanides C, Norman JT. Progressive renal disease: the chronic hypoxia hypothesis. Kidney Int Suppl. 1998;65:S74–S78.
4. Williamson JR, Chang K, Frangos M, Hasan KS, Ido Y, Kawamura T, Nyengaard JR, van den Enden M, Kilo C, Tilton RG. Hyperglycemic pseudohypoxia and diabetic complications. Diabetes. 1993;42:801–813.
5. Friederich-Persson M, Thörn E, Hansell P, Nangaku M, Levin M, Palm F. Kidney hypoxia, attributable to increased oxygen consumption, induces nephropathy independently of hyperglycemia and oxidative stress. Hypertension, 2013;62:914–919.
6. Friederich-Persson M, Persson P, Hansell P, Palm F. Deletion of uncoupling Protein-2 reduces renal mitochondrial leak respiration, intrarenal hypoxia and proteinuria in a mouse model of type 1 diabetes. Acta Physiol (Oxf). 2018;223:e13058.
7. Crunkhorn S. Mitochondrial uncoupler reverses diabetes. Nat Rev Drug Discov. 2014;13:885.
8. Abulizi A, Perry RJ, Camporez JPG, Jurczak MJ, Petersen KF, Aspichueta P, Shulman GI. A controlled-release mitochondrial protonophore reverses hypertriglyceridemia, nonalcoholic steatohepatitis, and diabetes in lipodystrophic mice. FASEB J. 2017;31:2916–2924.
9. Grundlingh J, Dargan PI, El-Zanfaly M, Wood DM. 2,4-dinitrophenol (DNP): a weight loss agent with significant acute toxicity and risk of death. J Med Toxicol. 2011;7:205–212.
10. Anders HJ, Huber TB, Isermann B, Schiffer M. CKD in diabetes: diabetic kidney disease versus nondiabetic kidney disease. Nat Rev Nephrol. 2018;14:361–377.
11. Le Page LM, et al. Increasing pyruvate dehydrogenase flux as a treatment for diabetic cardiomyopathy: a combined 13C hyperpolarized magnetic resonance and echocardiography study. Diabetes. 2015;64:2735–2743.
12. Stacpoole PW, Greene YJ. Dichloroacetate. Diabetes Care. 1992;15:785–791.
13. Qi W, Keenan HA, Li Q, Ishikado A, Kannt A, Sadowski T, Yorek MA, Wu IH, Lockhart S, Coppey LJ, Pfenninger A, Liew CW, Qiang G, Burkart AM, Hastings S, Pober D, Cahill C, Niewczas MA, Israelsen WJ, Tinsley L, Stillman IE, Amenta PS, Feener EP, Vander Heiden MG, Stanton RC, King GL. Pyruvate kinase M2 activation may protect against the progression of diabetic glomerular pathology and mitochondrial dysfunction. Nat Med. 2017;23:753–762.
14. Davis ME. Effect of chloroacetic acids on the kidneys. Environ Health Perspect. 1986;69:209–214.
15. Lewis AJ, Miller JJ, McCallum C, Rider OJ, Neubauer S, Heather LC, Tyler DJ. Assessment of metformin-induced changes in cardiac and hepatic redox state using hyperpolarized[1-13C]pyruvate. Diabetes. 2016;65:3544–3551.
16. Madiraju AK, Erion DM, Rahimi Y, Zhang XM, Braddock DT, Albright RA, Prigaro BJ, Wood JL, Bhanot S, MacDonald MJ, Jurczak MJ, Camporez JP, Lee HY, Cline GW, Samuel VT, Kibbey RG, Shulman GI. Metformin suppresses gluconeogenesis by inhibiting mitochondrial glycerophosphate dehydrogenase. Nature. 2014;510:542–546.
17. Qi H, Nielsen PM, Schroeder M, Bertelsen LB, Palm F, Laustsen C. Acute renal metabolic effect of metformin assessed with hyperpolarised MRI in rats. Diabetologia, 2017;61:445–454.
18. Laustsen C, Østergaard JA, Lauritzen MH, NØrregaard R, Bowen S, SØgaard LV, Flyvbjerg A, Pedersen M, Ardenkjaer-Larsen JH. Assessment of early diabetic renal changes with hyperpolarized [1-13C]pyruvate. Diabetes Metab Res Rev. 2013;29:125–129.
19. Laustsen C, LipsØ K, Ostergaard JA, NØrregaard R, Flyvbjerg A, Pedersen M, Palm F, Ardenkjær-Larsen JH. Insufficient insulin administration to diabetic rats increases substrate utilization and maintains lactate production in the kidney. Physiol Rep, 2014; 2. pii: e12233.
20. Laustsen C, Lycke S, Palm F, Østergaard JA, Bibby BM, NØrregaard R, Flyvbjerg A, Pedersen M, Ardenkjaer-Larsen JH. High altitude may alter oxygen availability and renal metabolism in diabetics as measured by hyperpolarized [1-13C]pyruvate magnetic resonance imaging. Kidney Int, 2013;86:67–74.
21. Laustsen C, Nielsen PM, NØrlinger TS, Qi H, Pedersen UK, Bertelsen LB, Østergaard JA, Flyvbjerg A, Ardenkjær-Larsen JH, Palm F, StØdkilde-JØrgensen H. Antioxidant treatment attenuates lactate production in diabetic nephropathy. Am J Physiol Renal Physiol. 2017;321:192–F199.
22. Friederich M, Fasching A, Hansell P, Nordquist L, Palm F. Diabetes-induced up-regulation of uncoupling protein-2 results in increased mitochondrial uncoupling in kidney proximal tubular cells. Biochim Biophys Acta, 2008;1777:935–940.
23. Morze CV, Allu PKR, Chang GY, Marco-Rius I, Milshteyn E, Wang ZJ, Ohliger MA, Gleason CE, Kurhanewicz J, Vigneron DB, Pearce D. Non-invasive detection of divergent metabolic signals in insulin deficiency vs. insulin resistance in vivo. Sci Rep. 2018;8:2088.
24. Mills EJ, Thorlund K, Ioannidis JP. Calculating additive treatment effects fromqa multiple randomized trials provides useful estimates of combination therapies. J Clin Epidemiol. 2012;65:1282–1228.
25. Breyer MD, Susztak K. Developing treatments for chronic kidney disease in the 21st century. Semin Nephrol. 2016;36:436–447.
26. Navarro-González JF, Mora-Fernández C, Muros de Fuentes M, Chahin J, Mández ML, Gallego E, Macía M, del Castillo N, Rivero A, Getino MA, García P, Jarque A, García J. Effect of pentoxifylline on renal function and urinary albumin excretion in patients with diabetic kidney disease: the PREDIAN trial. J Am Soc Nephrol. 2015;26:220–229.
27. Kasznicki J, Sliwinska A, Drzewoski J. Metformin in cancer prevention and therapy. Ann Transl Med. 2014;2:57.
28. Chang YT, Tsai HL, Kung YT, Yeh YS, Huang CW, Ma CJ, Chiu HC, Wang JY. Dose-dependent relationship between metformin and colorectal cancer occurrence among patients with type 2 diabetes-a nationwide cohort study. Transl Oncol. 2018;11:535–541.
29. Aggarwal R, Vigneron DB, Kurhanewicz J. Hyperpolarized 1-[13C]-pyruvate magnetic resonance imaging detects an early metabolic response to androgen ablation therapy in prostate cancer. Eur Urol. 2017;72:1028–1029.
30. Laustsen C. Hyperpolarized renal magnetic resonance imaging: potential and pitfalls. Front Physiol. 2016;7:72.
31. Nielsen PM, Eldirdiri A, Bertelsen LB, JØrgensen HS, Ardenkjaer-Larsen JH, Laustsen C. Fumarase activity: an in vivo and in vitro biomarker for acute kidney injury. Sci Rep. 2017;7:40812.
32. Nielsen PM, Laustsen C, Bertelsen LB, Qi H, Mikkelsen E, Kristensen ML, NØrregaard R, StØdkilde-JØrgensen H. In situ lactate dehydrogenase activity: a novel renal cortical imaging biomarker of tubular injury? Am J Physiol Renal Physiol. 2017;312:F465–F473.
33. Rosset A, Spadola L, Ratib O. OsiriX: an open-source software for navigating in multidimensional DICOM images. J Digit Imaging. 2004;17:205–216.
34. Gnaiger E. Mitochondrial Pathways and Respiratory Control: An Introduction to OXPHOS Analysis. 4th ed. Axams Austria: OROBOROS MiPNet Publications; 2014.